Climate Dynamics (2021) 56:3569–3579
https://doi.org/10.1007/s00382-021-05654-7

ENSO evolution asymmetry: EP versus CP El Niño

Mingcheng Chen[1] · **Tim Li**[1,2]

Received: 16 May 2019 / Accepted: 15 January 2021 / Published online: 2 March 2021

Abstract
Through an oceanic mixed-layer heat budget analysis, the dominant processes contributing to the largest decay rate (− 0.37 °C/mon) in EP El Nino, the moderate delay rate (− 0.22 °C/mon) in CP El Nino and the smallest decay rate (0.13 °C/mon) in La Nina, are identified. The result shows that both dynamic (wind induced equatorial ocean waves and thermocline changes) and thermodynamic (net surface solar radiation and latent heat flux changes) processes contribute to a fast decay and thus phase transition in EP El Niño composite, whereas the thermodynamic process has less effect on the decay rate for both CP El Niño and La Niña due to the westward shift of sea surface temperature anomaly (SSTA) centers. Thus, the difference in surface wind stress forcing is critical in contributing to evolution asymmetry between CP El Niño and La Niña, while the difference in both the wind stress and heat flux anomalies contribute to evolution asymmetry between EP El Niño and La Niña. It is interesting to note that El Nino induced anomalous anticyclone over the western North Pacific is stronger and shifts more toward the east during EP El Niño than during CP El Niño, while compared to CP El Niño, the center of an anomalous cyclone during La Niña shifts further to the west. As a consequence, both EP and CP El Niño decay fast and transform into a La Niña episode in the subsequent year, whereas La Niña has a much slower decay rate and re-develops in the second year.

Keywords ENSO · Evolution asymmetry · Anomaly GCM experiments · Western north pacific circulation anomaly response

1 Introduction

The El Niño-Southern Oscillation (ENSO) is the most prominent interannual mode in the tropics (Philander 1990; Trenberth et al. 1998; Wallace et al. 1998; Latif et al. 1998; Alexander et al. 2002). As the positive and negative aspects of ENSO events, El Niño exhibits a positive sea surface temperature anomaly (SSTA) in the equatorial central and eastern Pacific (CP and EP), whereas there is a negative SSTA occurred in the La Niña mature winter. The observational fact and model experiment results have shown that La Niña is not a mirror image of El Niño, and asymmetric features have been clearly seen in both amplitude (Burgers and Stephenson 1999; An and Jin 2004; Su et al. 2010; Chen et al. 2015) and evolution (Kessler 2002; Larkin and Harrison 2002; Okumura and Deser 2010; Dommenget et al. 2013; McGregor et al. 2013; Chen et al. 2016; Chen and Li 2018) between El Niño and La Niña.

In our previous study (Chen et al. 2016), we conducted an oceanic mixed-layer heat budget analysis to understand the cause of El Nino and La Nina evolution asymmetry. It was found that different from many previous studies that emphasized only the role of wind stress asymmetry, both the dynamic (i.e., wind stress asymmetry) and thermodynamic (i.e., surface shortwave radiative and latent heat flux asymmetry) processes are important in causing the El Niño-La Niña evolution asymmetry. During El Niño mature winter,

✉ Mingcheng Chen
mingchengchen@126.com

Tim Li
timli@hawaii.edu

[1] Key Laboratory of Meteorological Disaster, Ministry of Education (KLME)/Joint International Research Laboratory of Climate and Environmental Change (ILCEC)/Collaborative Innovation Center On Forecast and Evaluation of Meteorological Disasters (CIC-FEMD), Nanjing University of Information Science and Technology, Nanjing 210044, China

[2] International Pacific Research Center and Department of Atmospheric Sciences, School of Ocean and Earth Science and Technology, University of Hawaii at Manoa, Honolulu, HI 96822, USA

positive SSTA in EP induces an anomalous anticyclone over the Western North Pacific (hereafter WNPAC) through local air-sea thermodynamic feedback (Wang et al. 2000) and atmospheric moist enthalpy advection (Wu et al. 2017a, b; Li et al. 2017). Easterly anomalies south of the WNPAC trigger upwelling Kelvin waves propagating eastward, which can help El Niño decay fast. In contrast, anomalous cyclone (WNPC) is weaker and tends to shift west of the Philippine in La Niña mature phase (Wu et al. 2010). Thus, westerly anomalies south of the WNPC are weaker and shift westward, which lead to a slow decay. It is worth noting that, due to the asymmetry of SSTA pattern between El Niño and La Niña, the negative cloud-SST and evaporation-SST feedbacks becomes stronger in El Niño than in La Niña. Due to the distinctive decaying rates between El Nino and La Nina composites, El Niño decays much faster and transitions into a cold anomaly by summer of the second year, whereas La Niña decays slowly and remains a negative SSTA. As both Bjerknes thermocline feedback and zonal adjective feedback are strongest in northern fall (Li 1997), this season-dependent coupled instability leads to the growth of the remaining weak cold SSTA in both El Nino and La Nina composite and develops into a La Nina episode by the end of the second year.

However, EP and CP El Niño were not separate and were summed together as a single El Nino group in Chen et al. (2016). A natural question is what is the difference between EP and CP El Nino? Figure 1 shows the time evolutions of equatorial SSTA among EP El Niño, CP El Niño, and La Niña. The result shows that EP El Niño has a larger SSTA amplitude (more than 2 °C) with a center located in 120°W (Fig. 1a), while both CP El Niño and La Niña have weaker SSTA intensity (about 1 °C and − 1 °C, respectively) and tend to shift westward (around 150°W) in their mature phases (Fig. 1b, c). In the second year, both EP and CP El Niño have fast decaying processes and transform into La Niña episode, but La Niña has a slow decay and remains the negative SSTA throughout the year.

Thus, an important dynamic question that needs to be addressed is why CP El Niño also has a rapid decay and transforms into La Niña by the end of the second year, even though wind stress and heat flux anomaly responses could be very different between EP and CP El Niño. Given that the location of SSTA center during CP El Nino shifts even further westward compared to La Nina, the heat flux anomaly asymmetry between CP El Niño La Niña should be minor. Therefore, it is likely that the ocean dynamics associated with the wind stress forcing may be important in contributing to the fast decaying of CP El Niño after its peak phase.

The objective of this study is to reveal key physical processes that give rise to the distinctive evolutions among EP El Niño, CP El Niño, and La Niña. The remaining

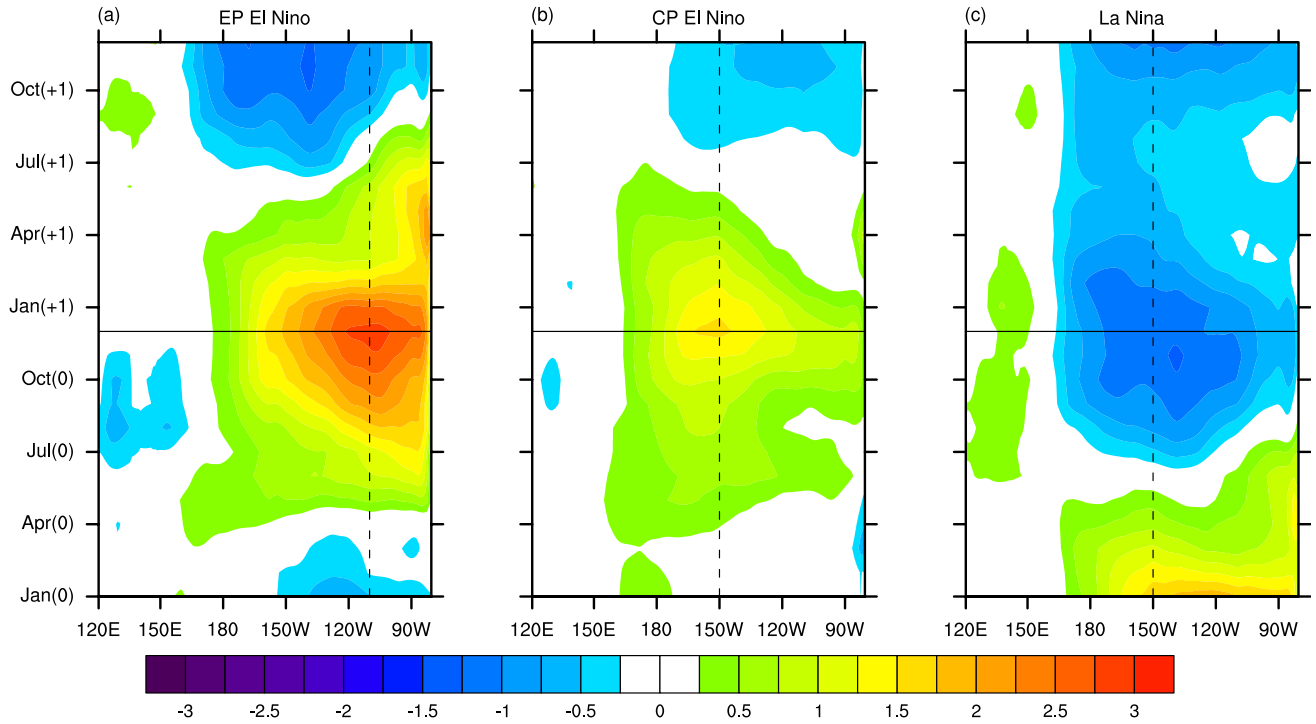

Fig. 1 Temporal evolutions of sea surface temperature anomaly (SSTA) for composite **a** EP El Niño (including 1982, 1997, and 2006 El Niños), **b** CP El Niño (including 1991, 1994, 2002, 2004, and 2009 El Niños), and **c** La Niña (including 1983/1984, 1995/1996, 1998/1999, 2007/2008, and 2010/2011 La Niñas) along the equator (5°N–5°S; unit: °C)

part of this paper is organized as follows. A description of datasets and oceanic mixed-layer heat budget analysis is given in Sect. 2. Sections 3 and 4 discuss the dynamic and thermodynamic processes in causing distinctive evolutions among EP El Niño, CP El Niño, and La Niña. Asymmetric wind effect between CP El Niño and La Niña is given in Sect. 5. Finally, a conclusion and discussion are given in the last section.

2 Datasets and methods

In this study, the primary ocean reanalysis datasets are derived from Simple Ocean Data Assimilation version 2.1.6 (SODA v2.1.6; Carton and Giese 2008), and NCEP Global Ocean Data Assimilation System (GODAS; Saha et al. 2006). The surface heat flux and atmospheric field datasets are mainly from the WHOI Objectively Analyzed Air-Sea Fluxes (OAFlux; Yu et al. 2008), and the NCEP reanalysis version 2 (NCEP v2; Kanamitsu et al. 2002). The observed SST, precipitation, and OLR datasets are from the Extended Reconstructed Sea Surface Temperature version 3b (ERSST v3b; Smith et al. 2008), the Climate Prediction Center (CPC) Merged Analysis of Precipitation (CMAP; Xie and Arkin 1997), and the National Oceanic and Atmospheric Administration (NOAA; Liebmann and Smith 1996), respectively.

Following Li et al. (2002), we conduct an oceanic mixed-layer heat budget analysis to understand the fundamental processes in causing the distinctive decaying rates among EP El Niño, CP El Niño and La Niña. The mixed-layer temperature anomaly tendency equation may be written as

$$\begin{aligned}\frac{\partial \mathbf{T}'}{\partial \mathbf{t}} &= -\left(\mathbf{u}'\partial\overline{\mathbf{T}}/\partial\mathbf{x} + \overline{\mathbf{u}}\partial\mathbf{T}'/\partial\mathbf{x} + \mathbf{u}'\partial\mathbf{T}'/\partial\mathbf{x}\right) \\ &\quad - \left(\mathbf{v}'\partial\overline{\mathbf{T}}/\partial\mathbf{y} + \overline{\mathbf{v}}\partial\mathbf{T}'/\partial\mathbf{y} + \mathbf{v}'\partial\mathbf{T}'/\partial\mathbf{y}\right) \\ &\quad - \left(\mathbf{w}'\partial\overline{\mathbf{T}}/\partial\mathbf{z} + \overline{\mathbf{w}}\partial\mathbf{T}'/\partial\mathbf{z} + \mathbf{w}'\partial\mathbf{T}'/\partial\mathbf{z}\right) \\ &\quad + \frac{\mathbf{Q}'_{\mathbf{net}}}{\boldsymbol{\rho}\mathbf{C}_{\mathbf{P}}\mathbf{H}} + \mathbf{R}\end{aligned}$$

The detailed description of tendency equation and parameters can be seen from Chen et al. (2016). Figure 2 shows the heat budget analysis result during the decaying phase (January–June in the second year) of EP El Niño, CP El Niño and La Niña averaged in the equatorial CP and EP region (5°N–5°S, 180°–80°W). It is seen that EP El Niño has the largest decaying rate (– 0.37 °C/month), while CP El Niño has a negative temperature anomaly tendency weaker than EP El Niño (– 0.22 °C/month), and La Niña has the weakest decaying rate in its decaying phase (0.13 °C/month). Both dynamic and thermodynamic processes are attributed to the distinctive decaying rates. In the dynamic terms, the major contributor are both the anomalous zonal advection term and the vertical entrainment term, while in the thermodynamic terms, the major contributors are both shortwave radiation term and latent heat flux term. In the following sections, we will discuss the dynamic and thermodynamic processes, respectively.

3 Dynamic processes in causing distinctive evolutions among EP El Niño, CP El Niño, and La Niña

The oceanic mixed-layer heat budget analysis result illustrates that, in the dynamic processes, it is the propagation of equatorial waves triggered by the wind field that induced the distinctive decaying rates. Thus, the distinctive wind responses over the WNP to ENSO forcing may exert a key effect on the zonal oceanic current difference among EP El Niño, CP El Niño and La Niña in their decaying phases. Figure 3 shows the composite 850 hPa wind, SST and precipitation anomalies in the mature winter (DJF). It can be seen that there are twin cyclonic couplets associated with warm SSTA (positive convective heating anomalies) in the equatorial EP, and a large-scale anomalous WNPAC, with its eastern edge can be extended to the dateline (Fig. 3a, b). Easterly wind anomalies south of the anticyclone can stimulate oceanic upwelling Kelvin waves propagating eastward, thus lead to a fast decay of warm SSTA in the equatorial EP. In the composite CP El Niño mature winter, an off-equatorial anomalous anticyclone also occurred west of 150°E, which is only weaker than that in the composite EP El Niño (Fig. 3c, d). To the south of the anticyclone, there are still anomalous easterly winds along the equatorial WP, which can lead to a fast decaying phase in the following decaying spring. Due to the anticyclonic circulation in the composite CP El Niño has a smaller size and weaker intensity than that in the composite EP El Niño, the anomalous zonal advection is a bit weaker in the decaying phase of CP El Niño (Fig. 2a, b). In contrast, an anomalous cyclone associated with La Niña forcing tends to shift more westward compared to the anticyclone in the composite El Niño, which has a center located in the South China Sea (Fig. 3e, f). It implies that there are easterly wind anomalies, rather than westerly wind anomalies, occurred along the equatorial WP. Due to the lack of the anomalous westerly wind forcing, a much weaker damping rate appeared in the decaying phase of composite La Niña events (Fig. 2c). Furthermore, the distinctive features of zonal wind along the equatorial WP are still existed in the following decaying spring (figure not shown), thus the distinctive damping rates will be maintained in the decaying phase of EP El Niño, CP El Niño and La Niña composite.

For the different wind forcing over the WNP, the thermocline depth anomalies exhibited different evolution

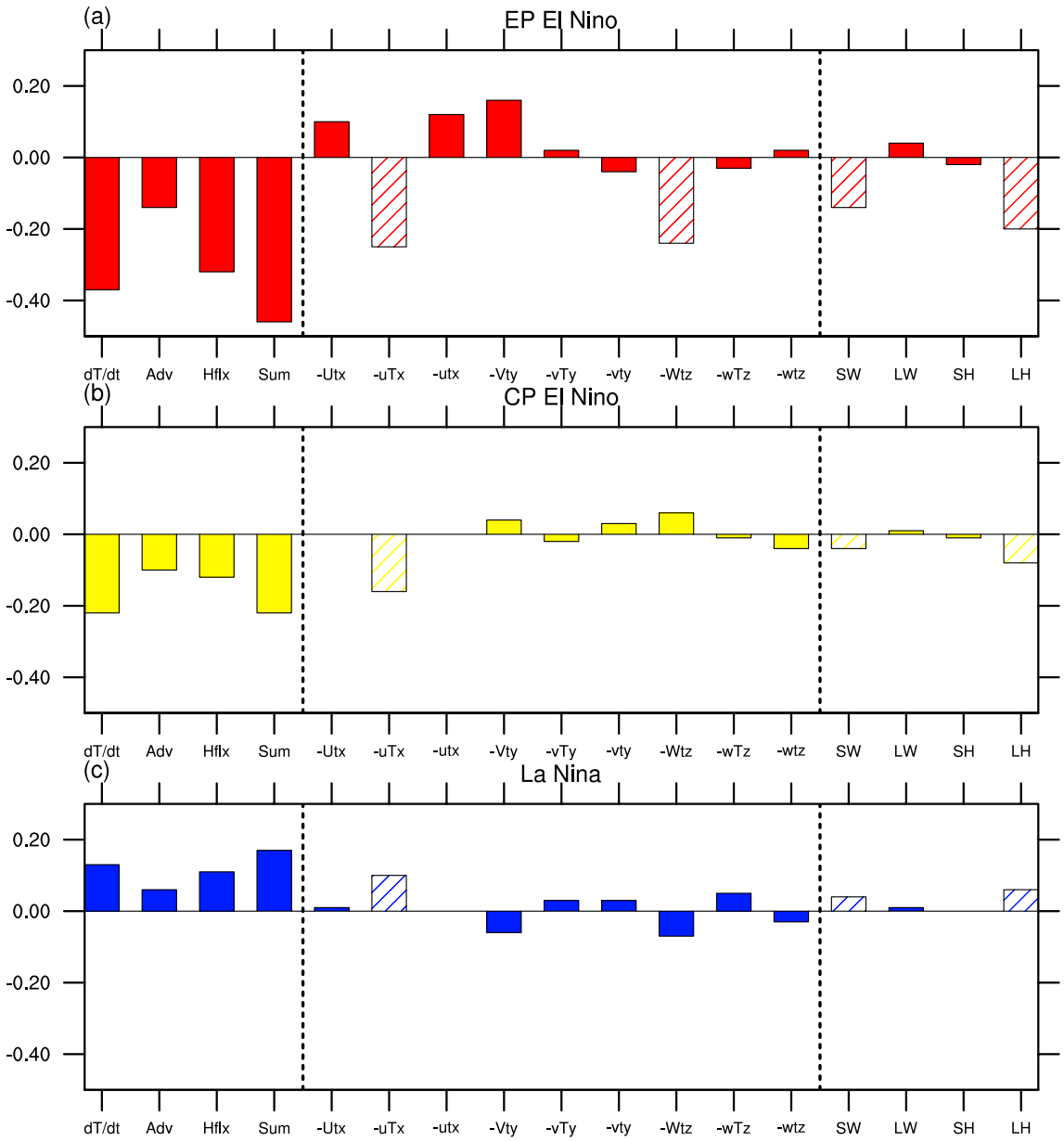

Fig. 2 Composite mixed-layer temperature anomaly (MLTA) heat budget analysis during the decaying phase (January–June in the second year) of **a** EP El Niño, **b** CP El Niño and **c** La Niña averaged in the equatorial eastern Pacific (EP; 180°–80°W, 5°S–5°N; °C/month). The values are based on the ensemble average of two ocean reanalysis datasets (SODA v2.1.6 and GODAS), and two surface heat flux products (OAFlux and NCEP R2)

features between the EP El Niño, CP El Niño and La Niña in the second year (Fig. 4). For the EP El Niño composite (left panel of Fig. 4), there is a large negative thermocline depth anomaly in the tropical western and central Pacific, and its eastern edge has reached 130°W in mature winter (Fig. 4a). In the following decaying spring (Fig. 4d, g), the strong negative signal continues strengthening as its center propagates eastward. As a result, positive thermocline depth anomaly in the equatorial EP is replaced by negative one in the second half of the second year (Fig. 4j, m). For the CP El Niño composite (middle panel of Fig. 4), although the negative thermocline depth anomaly is weaker than that in the EP El Niño, it can penetrate into the equatorial EP in later of the second year as well (Fig. 4n). Therefore, CP El Niño translates in to a La Niña episode. In contrast, due to the lack of the westerly anomaly forcing, the positive thermocline anomaly remains in the equatorial WP (west of 180°) in the La Niña composite (right panel of Fig. 4), and the negative one cannot change the sign in the equatorial EP throughout

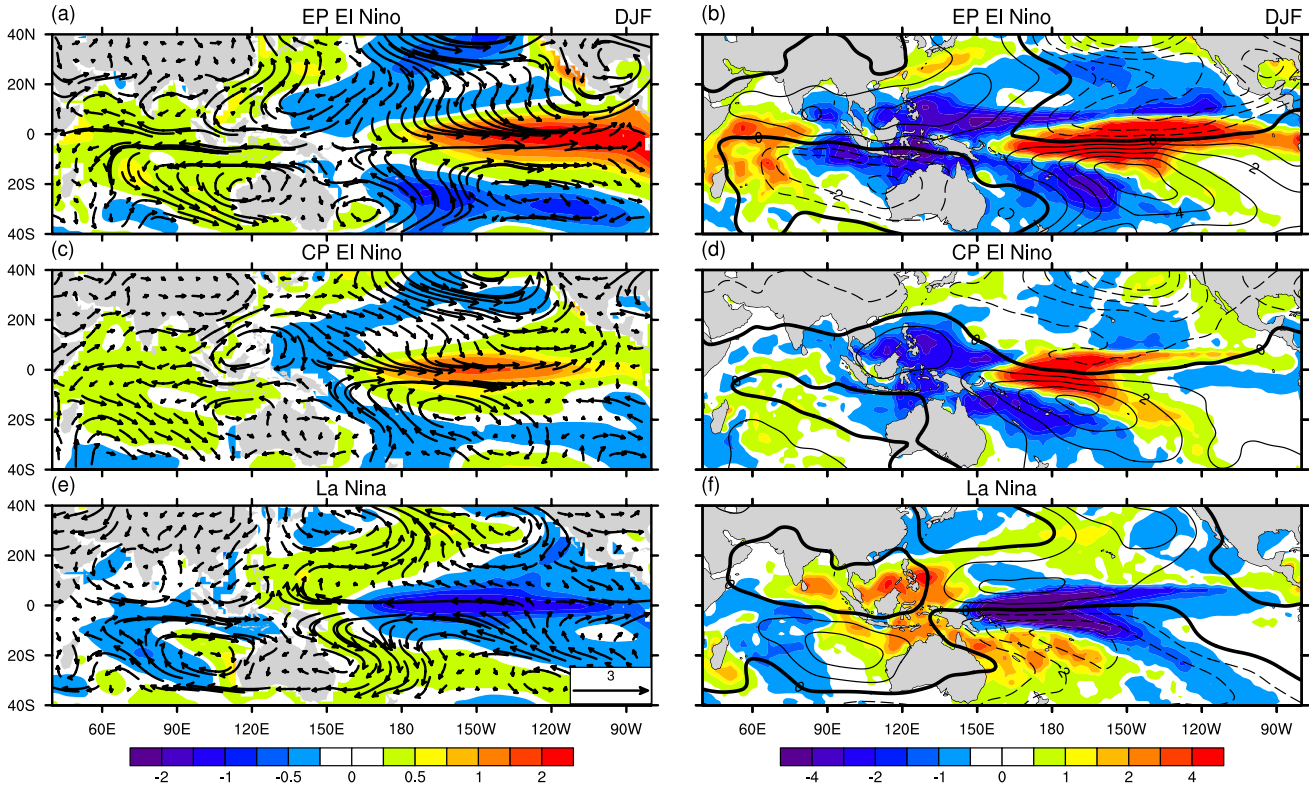

Fig. 3 Composite (left panel) SSTA (shading; unit: °C) and 850 hPa wind anomalies (vectors; unit: m/s), and (right panel) precipitation (shading; unit: mm/day) and stream function anomalies (contours; unit: 10^6 m^2/s) for **a**, **b** EP El Niño, **c**, **d** CP El Niño, and **e**, **f** La Niña in the mature winter (DJF)

the year + 1. As a result, La Niña has a much slower decaying process than both EP and CP El Niño.

Figure 5 illustrates the composite equatorial zonal ocean currents and temperature anomalies for EP El Niño, CP El Niño, and La Niña in the year + 1. It can be clearly seen that, both EP and CP El Niño have stronger westward geostrophic currents (negative thermocline depth anomaly induced) at the upper ocean in the earlier half of year + 1. The westward currents anomalies advect climatological mean SST, which lead to an anomalous cold zonal advection. As a result, the cold subsurface water can easily spread into the equatorial EP in the end. In contrast, for the La Niña composite (right panel of Fig. 5), the eastward geostrophic currents are weaker due to lack of westerly anomalies forcing over the equatorial WP. Therefore, the anomalous warm subsurface water is locked in the WP, while La Niña decays slowly and keeps its sign in the end of the second year.

4 Thermodynamic processes in causing distinctive evolutions among EP El Niño, CP El Niño, and La Niña

In additional to the wind effect, the local heat flux forcing also has an effect on the SSTA change in the equatorial EP. Previous study illustrated that the asymmetric thermodynamic forcing is as important as the asymmetric dynamic forcing during ENSO decaying phase, and the major contributors are shortwave radiation and latent heat flux (Chen et al. 2016).

In warm oceans, a modest SSTA may induce deep convection in situ. The increased clouds tend to reduce the downward shortwave radiation and thus decrease the SST, which lead to a negative cloud-radiation-SST feedback between the atmosphere and ocean (Li et al. 2003). The composite OLR anomalies during the decaying phases of EP El Niño, CP El Niño, and La Niña are shown in the left panel of Fig. 6. In the EP El Niño composite (Fig. 6a), negative OLR anomaly occurs in the equatorial central and eastern Pacific, with a center located in 140°W. In contrast, due to the westward shift of SSTA in both CP El Niño and La Niña, the OLR anomalies tend to shift westward with centers around 180° (Fig. 6c, e). Note that the amplitude of SSTA in EP El Niño

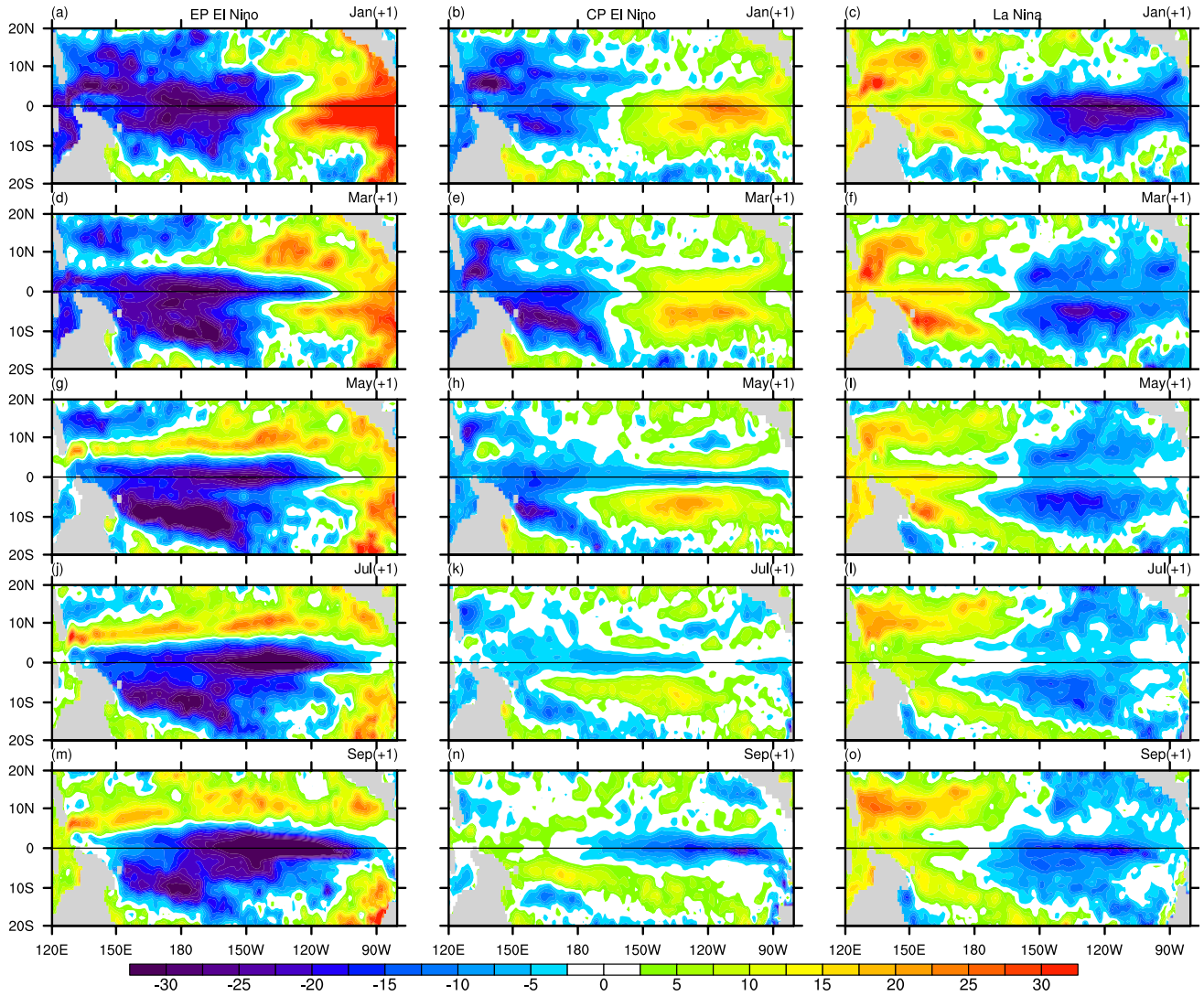

Fig. 4 Thermocline depth anomalies (shading; unit: m) for composite (left panel) EP El Niño, (middle panel) CP El Niño, and (right panel) La Niña in the second year

is two times as large as that in CP El Niño and La Niña (Fig. 1), thus a larger OLR anomaly occurred during EP El Niño decaying phase (Fig. 6a). For the EP El Niño composite, the negative shortwave radiation (or OLR) forcing can affect the equatorial EP SSTA in situ (180°–80°W), whereas it tends to shift more westward (150°E–150°W) for CP El Niño and La Niña composite. As a result, in the heat budget area (180°–80°W, 5°N–5°S), there is a large damping term of shortwave radiation in EP El Niño (– 0.14 °C/month), but much weaker in CP El Niño and La Niña (– 0.04 and 0.04 °C/month, respectively).

The asymmetry of the anomalous latent heat fluxes also has an impact on the distinctive decaying rates of EP El Niño, CP El Niño, and La Niña. And it is mainly attributed to the anomalous sea-air specific humidity difference (q_s–q_a; Chen et al. 2016). As the q_s–q_a field is proportional to local SST (Li and Wang 1994), a larger positive q_s–q_a anomaly is located in the equatorial EP during the decaying phase of EP El Niño. Meanwhile, the weaker q_s–q_a anomalies tend to shift westward with centers around 180° in both CP El Niño and La Niña, in a way similar to the cloud-radiation-SST feedback (right panel of Fig. 6). As a result, the surface latent heat term is larger in EP El Niño (– 0.2 °C/month), but much weaker in CP El Niño and La Niña (– 0.08 and 0.06 °C/month, respectively).

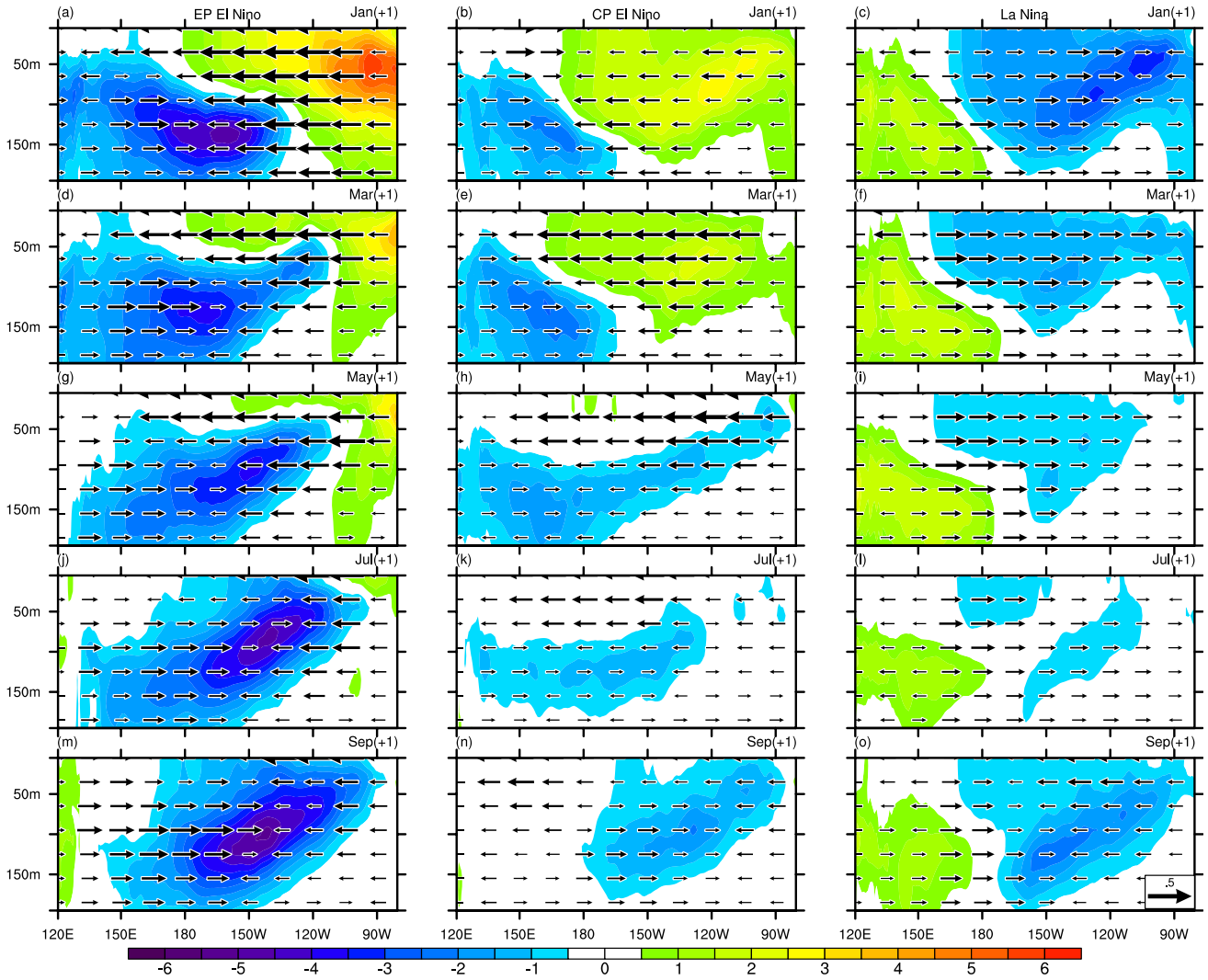

Fig. 5 Composite equatorial (2°S–2°N) ocean anomalous zonal currents (vectors; unit: m/s) and temperature anomalies (shading; unit: °C) for (left panel) EP El Niño, (middle panel) CP El Niño, and (right panel) La Niña in the second year

5 Asymmetric wind effect between CP El Niño and La Niña

During the mature phases of ENSO events, EP El Niño has stronger amplitude than CP El Niño due to farther eastward SSTA. As a result, there is a large-scale WNPAC which leads to a fast decay of EP El Niño. Meanwhile, farther eastward SSTA can induce stronger local negative thermodynamic feedbacks (shortwave radiation and latent heat flux), which has a great impact on the fast decay of EP El Niño, either. On the contrary, both CP El Niño and La Niña have SSTA center located in the equatorial CP (around 150°W; Fig. 1b, c), thus thermodynamic feedbacks are comparable (Fig. 6c–f) and have little influence on the decaying process (Fig. 2b, c). As a result, the asymmetric evolution between CP El Niño and La Niña is primarily attributed to the dynamic processes. In the dynamic processes, the propagation of equatorial waves triggered by the wind field is the key factor. In the CP El Niño, the WNP is dominated by anticyclone, with its eastern edge located in 150°E. The easterly anomalies south of the anticyclone induce eastward upwelling Kelvin waves in equatorial WP, and the negative thermocline anomalies can penetrate into the EP rapidly. The eastward anomalous cold advection in the upper ocean can cool the original warm SSTA in the CP El Niño (middle panel of Figs. 2, 3, 4, 5). Otherwise, the anomalous WNPC in La Niña has a westward shift to the South China Sea, with its eastern edge located in 130°E, which has a westward shift of 20 longitude degrees compared to CP El Niño. As a result, it is dominated by anomalous anticyclone over the WNP. Due to lack of the anomalous westerly forcing, the negative thermocline anomalies in western Pacific is hard to extend eastward. There is a weaker warm ocean advection,

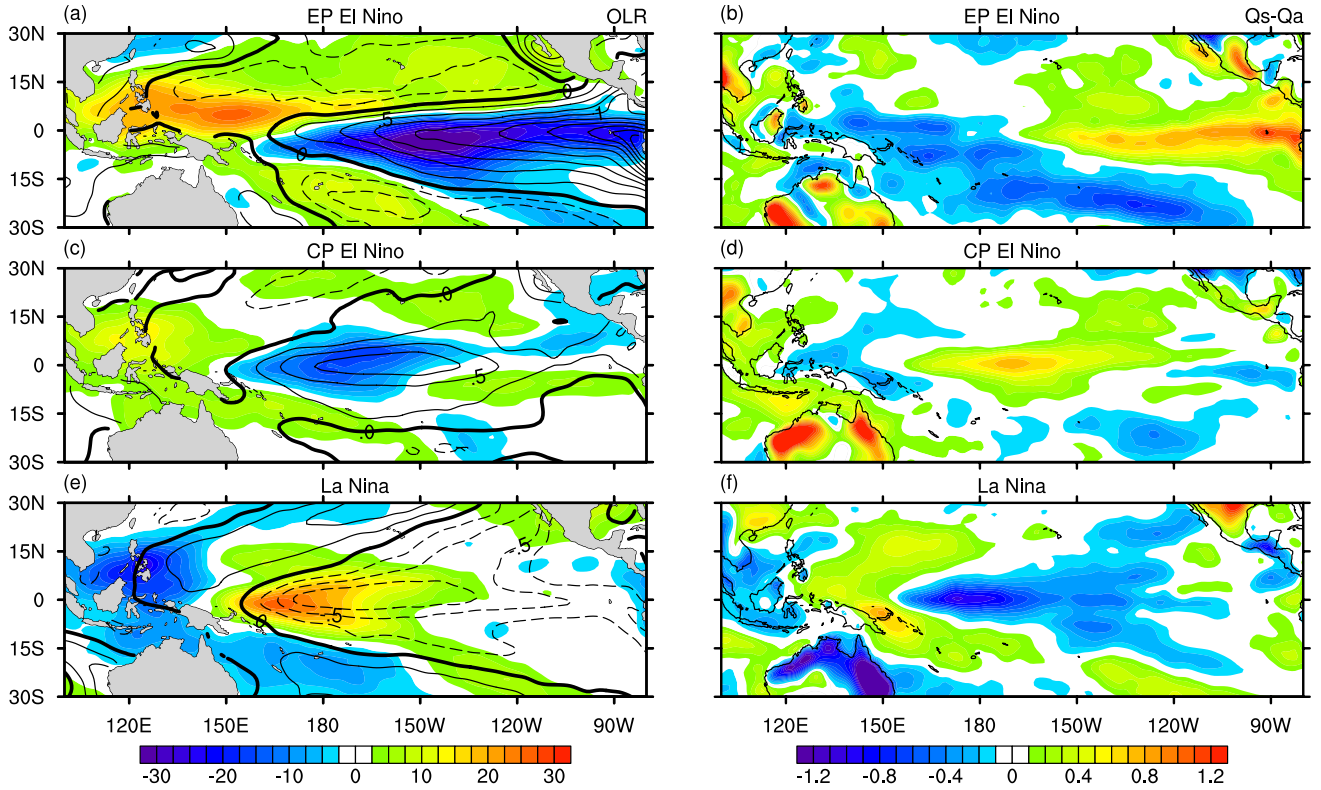

Fig. 6 Composite patterns of anomalous (left panel) OLR (shading; unit: W/m^2), sea surface temperature (contours; unit: °C) and (right panel) sea-air specific humidity difference (unit: g/kg) fields during the decaying phase (Jan–Jun in year + 1) of **a**, **b** EP El Niño, **c**, **d** CP El Niño and **e**, **f** La Niña

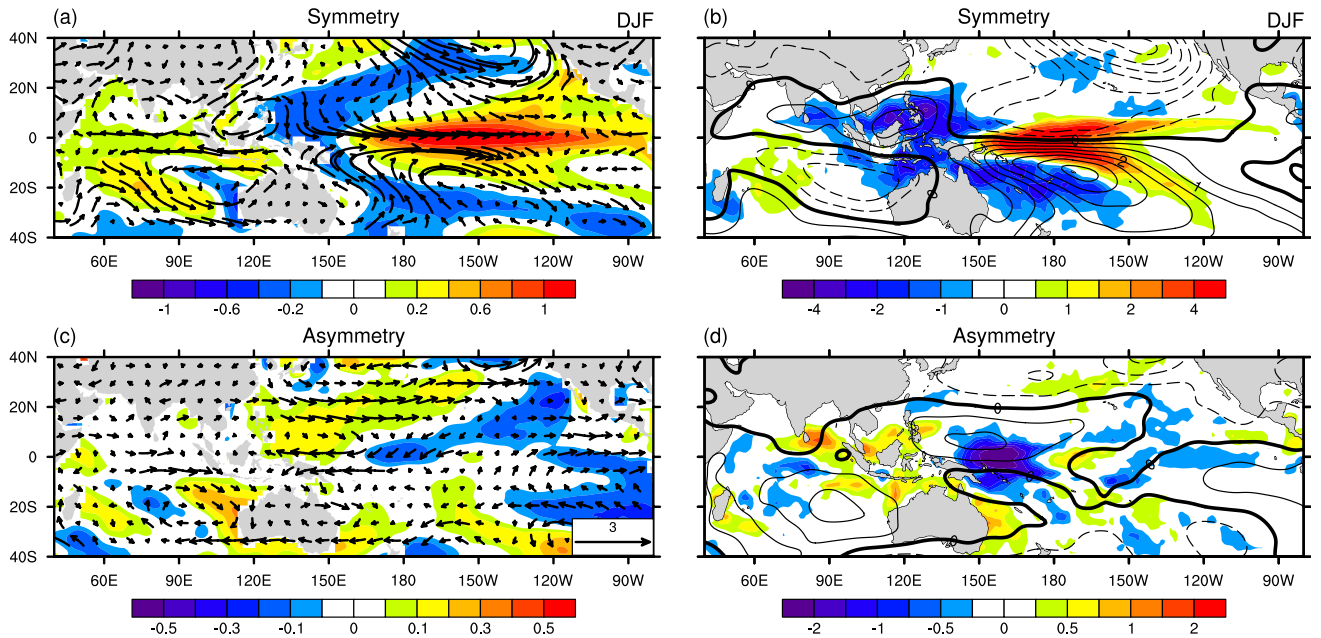

Fig. 7 Composite **a**, **b** normalized symmetric and **c**, **d** asymmetric components of (left panel) SSTA (shading; unit: °C) and 850 hPa wind anomalies (vectors; unit: m/s), and (right panel) precipitation (shading; unit: mm/day) and stream function anomalies (contours; unit: 0.5×10^6 m^2/s) between CP El Niño and La Niña in the mature winter (DJF). The symmetric component is obtained by half of difference of them, while the asymmetric component estimated by half of sum of them. The normalized components are calculated according to Niño-3.4 SSTA amplitude

and La Niña decays slowly (bottom panel of Figs. 2, 3; right panel of Figs. 4, 5).

In order to investigate the cause of atmospheric circulation asymmetry between CP El Niño and La Niña, we calculate the symmetric and asymmetric components of the 850 hPa wind field, SSTA and precipitation anomalies (Fig. 7). Considering that SSTA in CP El Niño is slightly stronger than that of La Niña, the normalized components calculated according to Niño-3.4 SSTA amplitude are given. It can be seen from the normalized symmetric component (Fig. 7a, b) that, during the mature winter of CP El Niño (La Niña), the positive (negative) SSTA center is located at 150°W. As result, the positive (negative) precipitation anomaly has a center west of the dateline. In response to the convection, there are twin cyclone (anticyclone) couplets in the off-equatorial CP region. The anomalous descending (ascending) motion region is over the Maritime Continent and WNP, where anomalous WNPAC (WNPC) can be clearly seen with its east edge reaches to 140°E. For the normalized asymmetric component (Fig. 7c, d), both CP El Niño and La Niña have zonal dipole patterns of SSTA along the equatorial WP and CP. Correspondingly, the anomalous convective heating also has an east–west dipole mode. Positive precipitation anomaly is located in Maritime Continent, while the negative one occurs around 160°E. The WNP region is dominated by anomalous anticyclone, and it can affect whole WNP, ranging from 120° E to 180°. It seems that the anomalous anticyclone is induced by the equatorial dipole heating pattern. We use anomaly GCM to further verify the heating effect as follows.

To study how the atmospheric wind responds to the symmetric and asymmetric precipitation anomalies under ENSO mature winter, an anomaly atmospheric GCM was used. This model was developed based on the Geophysical Fluid Dynamics Laboratory (GFDL) global spectral dry AGCM (Held and Suarez 1994). The detailed description of anomaly GCM can be referred to Jiang and Li (2005) and Li et al. (2006).

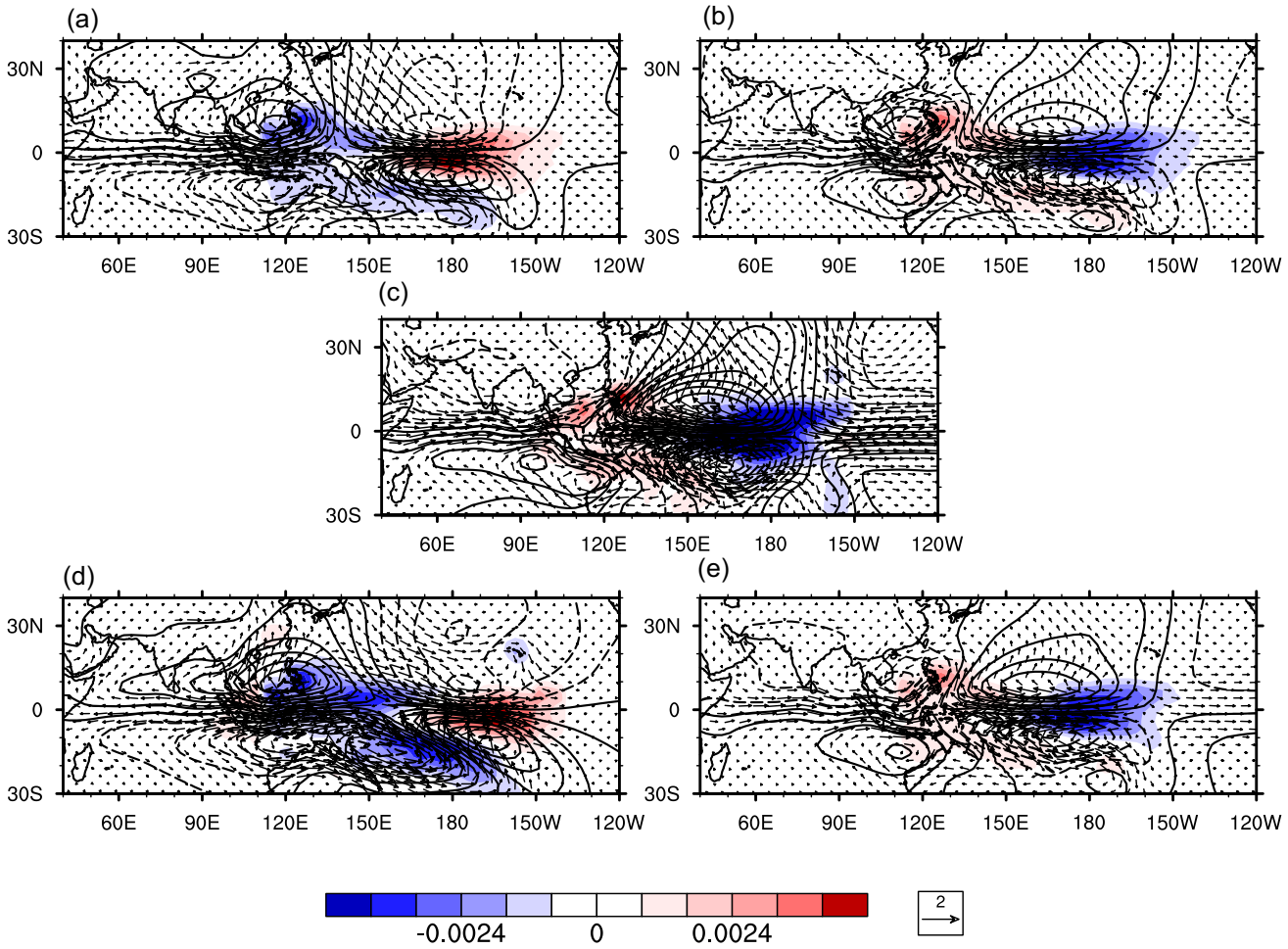

Fig. 8 The 850 hPa wind (vectors; unit: m/s) and stream function (contours; unit: 10^5 m^2 s^{-1}) anomalies simulated by anomaly AGCM respond to the (top panel) normalized symmetric, (middle panel) asymmetric, and (bottom panel) original precipitation field during ENSO mature winter (DJF). The diabatic heating rates (shading; unit: K day^{-1}) are also shown

In this study, the observed winter (DJF) mean state is specified as the model background state. The symmetric, asymmetric and total heating anomaly calculated based on observed precipitation anomaly field during ENSO mature winter are specified in the model. An idealized vertical profile with a maximum center in middle troposphere is specified for the diabatic heating anomaly.

The 850 hPa wind (vectors) and stream function (contours) anomalies simulated by anomaly AGCM respond to the normalized symmetric components of CP El Niño and La Niña diabatic heating (shading) are given (Fig. 8a, b). It is seen that the anomalous WNPAC and WNPC are symmetric. The eastern edge of WNPAC (WNPC) reaches to 140°E, which is similar to that in the observational fact (Fig. 7b). Figure 8c shows the wind field respond to the asymmetric component of heating, and there is an anomalous anticyclone over the whole WNP region (120°E–180°). The anomalous anticyclonic circulation enhances the intensity and extends the size of the WNPAC, while weakens the WNPC and leads to a westward shift. As a result, in the real forcing experiments (including both symmetric and asymmetric components), there is a stronger anomalous anticyclone over the WNP with its eastern edge extended to 150°E for the CP El Niño (Fig. 8d), while the anomalous cyclone is weaker with its eastern edge has a westward retreat for more than 20 degrees of longitude in the La Niña composite (Fig. 8e). And the simulation results are consistent with the observations (Fig. 3d, f).

6 Conclusion

The observational fact illustrated that during the mature winter of ENSO events, EP El Niño has larger SSTA amplitude with a center located in 120°W, while both CP El Niño and La Niña have weaker intensity of SSTA and shifts more westward to 150°W. The ocean mixed-layer temperature anomaly heat budget analysis result shows that EP El Niño has the largest decaying rate, while CP El Niño also has a negative tendency weaker than EP El Niño, and La Niña has the weakest damping rate. For the EP El Niño, both dynamic and thermodynamic processes are contributed to the fast decay. The former is related to wind response (anticyclone) over the WNP, whereas the latter is associated with negative cloud-radiation-SST and evaporation-SST feedbacks. Due to the westward shift of weaker SSTA, the thermodynamic damping effect is weaker in both CP El Niño and La Niña. It is the wind induced (WNPAC) equatorial wave effect (eastward propagating upwelling Kelvin waves) that contributes to the fast decaying process of CP El Niño. For the La Niña composite, due to lack of anomalous westerly forcing south of the WNPC, there is a slow decay and SSTA remains the negative sign in summer of the second year. Because both Bjerknes thermocline feedback and zonal advective feedback are strongest in northern fall, thus the weak SSTA starts to develop and reaches a peak in the following boreal winter. Both EP and CP El Niño transform into La Niña episode, but La Niña re-develops into another cold phase in the end of the second year.

By conducting a series of experiments using dry AGCM, the asymmetric wind effect between CP El Niño and La Niña is investigated. The model simulation result shows that it is the asymmetric component of convective heating that contributes to the wind field asymmetry. In the mature winter, the asymmetric component of SSTA is characterized by a zonal dipole mode, with positive anomaly over the WNP and negative one around the dateline along the equator. As a result, the asymmetric convective heating also represents a zonal dipole mode, which leads to an anomalous anticyclone over the WNP. The anomalous anticyclonic circulation enhances the intensity and extends the size of the WNPAC, while weakens the WNPC and leads to a westward shift. Therefore, the composite CP El Niño decays fast and transforms into a cold phase, but no phase change occurs in the La Niña composite.

Acknowledgements This work was supported by NSFC Grants 41630423, The National Key R&D Program of China 2019YFC1510004, NSF Grant AGS-2006553, and Jiangsu NSF Grant BK20180811. This is SOEST contribution number 11241, and IPRC contribution number 1506.

References

Alexander MA, Bladé I, Newman M, Lanzante JR, Lau N-C, Scott JD (2002) The atmospheric bridge: the influence of ENSO teleconnections on air-sea interaction over the global oceans. J Clim 15:2205–2231

An SI, Jin FF (2004) Nonlinearity and asymmetry of ENSO. J Clim 17:2399–2412

Burgers G, Stephenson DB (1999) The "'normality"' of El Niño. Geophys Res Lett 26:1027–1030

Carton JA, Giese BS (2008) A reanalysis of ocean climate using simple ocean data assimilation (SODA). Mon Weather Rev 136:2999–3017

Chen M, Li T (2018) Why 1986 El Niño and 2005 La Niña evolved different from a typical El Niño and La Niña. Clim Dyn. https://doi.org/10.1007/s00382-017-3852-1

Chen L, Li T, Yu Y (2015) Causes of strengthening and weakening of ENSO amplitude under global warming in four CMIP5 models. J Clim 28:3250–3274

Chen M, Li T, Shen X, Wu B (2016) Relative roles of dynamic and thermodynamic processes in causing evolution asymmetry between El Niño and La Niña. J Clim 29:2201–2220

Dommenget D, Bayr T, Frauen C (2013) Analysis of the non-linearity in the pattern and time evolution of El Niño southern oscillation. Clim Dyn 40:2825–2847

Held IM, Suarez MJ (1994) A proposal for the intercomparison of the dynamical cores of atmospheric general circulation models. Bull Am Meteorol Soc 75:1825–1830

Jiang XA, Li T (2005) Reinitiation of the boreal summer intraseasonal oscillation in the tropical Indian Ocean. J Clim 18:3777–3795
Kanamitsu M, Ebisuzaki W, Woollen J, Yang S-K, Hnilo JJ, Fiorino M, Potter GL (2002) NCEP-DOE AMIP-II reanalysis (R-2). Bull Amer Meteor Soc 83:1631–1643
Kessler WS (2002) Is ENSO a cycle or a series of events? Geophys Res Lett 29:2125. https://doi.org/10.1029/2002GL015924
Larkin NK, Harrison DE (2002) ENSO warm (El Niño) and cold (La Niña) event life cycles: ocean surface anomaly patterns, their symmetries, asymmetries, and implications. J Clim 15:1118–1140
Latif M, Anderson D, Barnett T et al (1998) A review of the predictability and prediction of ENSO. J Geophys Res 103:14375–14393
Li T (1997) Phase transition of the El Niño-Southern Oscillation: a stationary SST mode. J Atmos Sci 54:2872–2887
Li T, Wang B (1994) A thermodynamic equilibrium climate model for monthly mean surface winds and precipitation over the tropical Pacific. J Atmos Sci 51:1372–1385
Li T, Zhang Y-S, Chang C-P, Lu E, Wang D (2002) Relative role of dynamic and thermodynamic processes in the development of the Indian Ocean dipole: an OGCM diagnosis. Geophys Res Lett 29:2110. https://doi.org/10.1029/2002GL015789
Li T, Wang B, Chang CP, Zhang Y (2003) A theory for the Indian Ocean dipole–zonal mode. J Atmos Sci 60:2119–2135
Li T, Liu P, Fu X, Wang B (2006) Spatiotemporal structures and mechanisms of the tropospheric biennial oscillation in the Indo-Pacific warm ocean regions. J Clim 19:3070–3087
Liebmann B, Smith CA (1996) Description of a complete (interpolated) outgoing longwave radiation dataset. Bull Am Meteor Soc 77:1275–1277
McGregor S, Ramesh N, Spence P, England MH, McPhaden MJ, Santoso A (2013) Meridional movement of wind anomalies during ENSO events and their role in event termination. Geophys Res Lett 40:749–754
Okumura YM, Deser C (2010) Asymmetry in the duration of El Niño and La Niña. J Clim 23:5826–5843
Philander SGH (1990) El Niño, La Niña, and the Southern Oscillation. Academic Press, New York, p 293
Saha S, Nadiga S, Thiaw C et al (2006) The NCEP climate forecast system. J Clim 19:3483–3517
Smith RD, Dukowicz JK, Malone RC (1992) Parallel ocean general circulation modeling. Phsica D 60:38–61
Su J, Zhang R, Li T, Rong X, Kug J-S, Hong C-C (2010) Causes of the El Niño and La Niña amplitude asymmetry in the equatorial eastern Pacific. J Clim 23:605–617
Trenberth KE, Branstator GW, Karoly D et al (1998) Progress during TOGA in understanding and modeling global teleconnections associated with tropical sea surface temperatures. J Geophys Res 103:14291–14324
Wallace JM, Rasmusson EM, Mitchcell TP et al (1998) On the structure and evolution of ENSO-related climate variability in the tropical Pacific: lessons from TOGA. J Geophys Res 103:14241–14259
Wang B, Wu RG, Fu XH (2000) Pacific-East Asian teleconnection: how does ENSO affect East Asian climate? J Clim 13:1517–1536
Wu B, Li T, Zhou TJ (2010) Asymmetry of atmospheric circulation anomalies over the western North Pacific between El Niño and La Niña. J Clim 23:4807–4822
Wu B, Zhou TJ, Li T (2017a) Atmospheric dynamic and thermodynamic processes driving the western North Pacific anomalous anticyclone during El Niño. Part I: maintenance mechanisms. J Clim 30:9621–9635
Wu B, Zhou TJ, Li T (2017b) Atmospheric dynamic and thermodynamic processes driving the western North Pacific anomalous anticyclone during El Niño. Part II: Formation processes. J Clim 30:9637–9650
Xie P, Arkin PA (1997) Global precipitation: A 17-year monthly analysis based on gauge observations, satellite estimates, and numerical model outputs. Bull Am Meteor Soc 78:2539–2558
Yu L, Jin X, Weller RA (2008) Multidecade global flux datasets from the Objectively Analyzed air-sea Fluxes (OAFlux) Project: Latent and sensible heat fluxes, ocean evaporation, and related surface meteorological variables. Woods Hole Oceanographic Institution Tech. Rep. OA-2008–1, pp 64